Subwavelength-resolution direct writing using submicron-diameter fibers

Feng Tian (田 丰), Guoguang Yang (杨国光), Jian Bai (白 剑)*, Qiaofen Zhou (周巧芬), Changlun Hou (侯昌伦), Jianfeng Xu (徐建锋), and Yiyong Liang (梁宜勇)

State Key Laboratory of Modern Optical Instrumentation, Department of Optical Engineering, Zhejiang University, Hangzhou 310027, China

**E-mail: bai@zju.edu.cn*

Received May 11, 2009

A novel direct writing technique using submicron-diameter fibers is presented. This technique adopts contact mode in the process of writing, and submicron lines with different widths have been obtained. Experimental results demonstrate that the resolution of this technique can be smaller than the exposure wavelength of 442 nm, and 380-nm-wide line is achieved. In addition, the distribution of light fields in the photoresist layer is analyzed by finite-difference time-domain method.

OCIS codes: 220.4241, 110.4235, 140.3510, 310.6628.

doi: 10.3788/COL20100803.0326.

Direct writing techniques allow maskless definition of surface micro- and nano-structures. They are adopted to fabricate various optical devices with micro- and nano-structures, such as wire-grid polarizers[1], photon crystals[2], fiber Bragg gratings (FBGs)[3], and optical micro-electro-mechanical systems (MEMS)[4], etc. The popular direct writing techniques include laser direct writing[5,6] and electron beam direct writing[7]. The laser direct writing is a mature and reliable technique. Nevertheless, because of the diffraction limit, it is very difficult for laser direct writing to reach the subwavelength resolution. The electron beam direct writing can fabricate sub-100-nm structures, but its processes tend to be costly and inconvenient, so its applications are restricted in a narrow range.

Submicron-diameter fibers have attracted much attention on account of their favorable properties, such as tight optical confinement, low optical loss, high fraction of evanescent fields, and strong field enhancement[8−10]. All these excellent properties make the submicron-diameter fiber suitable for maskless lithography. Firstly, the tight optical confinement can provide the high exposure resolution. Secondly, the low optical loss and strong field enhancement ensure the exposure power. Thirdly, the high fraction of evanescent fields can be easily coupled into the photoresist layer. Based on these, we present a novel direct writing technique utilizing the submicron-diameter fibers in this letter. These fiber probes are used as an "inked pen", transferring a laser "ink" from the probe tip to a photoresist layer through direct contact. However, there are some differences between the submicron-diameter fiber probes for direct writing and the usual micro- and nano-fibers. The usual micro- and nano-fibers are used to fabricate a variety of micro- and nano-photonic components or devices, such as fiber gratings, Mach-Zehnder interferomenters (MZIs), filters, ring resonators, and knot lasers, etc.[11−15] In these applications, micro- and nano-fibers act as waveguides. Contrary to the uninterrupted micro- and nano-fibers, the submicron-diameter fiber probes are interrupted and serve as submicron-dimension point sources. Moreover, the submicron-diameter fiber probes not only can be used for direct writing but also are helpful for possible applications in nano-probe sensing, laser trapping, and laser scalpel for nano-sergery.

Figure 1(a) shows the scheme of direct writing using submicron-diameter fibers. A dilute photoresist (AZ MIR701) is spun onto a silicon substrate to obtain a 120-nm-thick photoresist layer. The silicon substrate is then placed at an XYZ translation stage driven by three high-precision motors with the resolution of 0.05 μm per pulse. The submicron-diameter fiber probe is fixed above the stage and a small angle is kept between the probe and the substrate plane. If the probe is perpendicular to the substrate, it will be curved by Van der Waals force during contact writing. Therefore, we adopt an almost parallel probe pose. A 442-nm He-Cd laser is selected as the light source and is coupled with the fiber through a microscope objective. Initially, the stage moves in the Z direction to approach the submicron-diameter fiber probe until the probe tip contacts with the photoresist layer. This process is monitored by the microscope camera. After alignment, the stage moves in the Y direction. Because of the contact mode during moving, the submicron-diameter fiber guides the light into photoresist layer and a narrow line is exposed. After writing this line, the stage moves a distance alone the X direction and repeats the above steps to write another line. Compared with near-field scanning optical microscopy (NSOM) direct writing[16], the submicron-diameter fiber direct writing has three remarkable advantages. Firstly, it does not need the control of the distance between probe and substrate during writing. Secondly, because the light power guided into the photoresist is larger than the near-field irradiation, the writing speed can be dramatically higher. Thirdly, using the motor for driving stage rather than piezoelectric ceramic can largely expand the writing area.

The main challenge of this direct writing technique is the fabrication of the submicron-diameter fiber probe.

 © 2010 Chinese Optics Letters

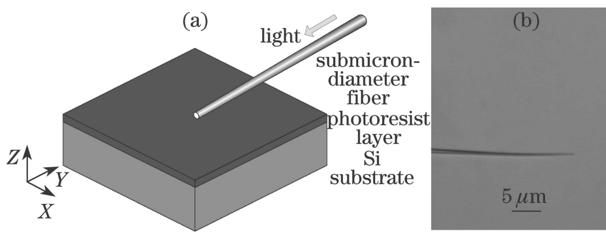

Fig. 1. (a) Scheme of direct writing using submicron-diameter fiber. Contact exposure is adopted during submicron-diameter fiber scanning on the photoresist layer. (b) Optical microscope image of a fiber probe fabricated by two-step process for direct writing. Its tip diameter is about 500 nm.

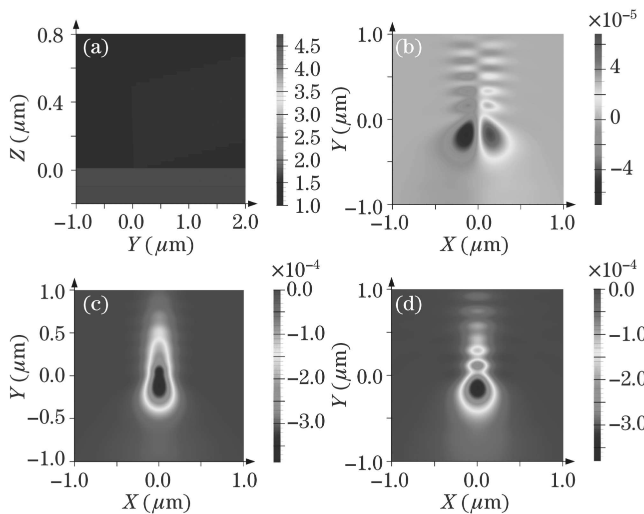

Fig. 2. (a) Index model of direct writing for FDTD simulation; (b) X, (c) Y, and (d) Z components of Poynting vector in the middle plane of the photoresist layer.

Usual silica micro- and nano-fibers are fabricated by flame-heated drawing of single-mode fibers[8]. Because of their length and flexibility, these micro- and nano-fibers cannot support themselves in the air. In order to increase its stiffness, an ideal micron-diameter fiber probe for direct writing must gradually change its diameter to a submicron tip. Here we report a two-step fabrication process of the submicron-diameter fiber probes. Firstly, while heated by a flame, the silica fiber is drawn to a taper with a diameter of about 3 μm. Then, we use the hydrofluoric (HF) acid solution to etch the taper until its diameter is reduced to submicron-dimension. Figure 1(b) shows an optical microscope image of a direct writing fiber probe with a tip diameter of about 500 nm.

We simulate the light fields within the photoresist layer using finite-difference time-domain (FDTD) method. This FDTD simulation is performed by "Lumerial FDTD Solutions", a special software. The index model for the simulation is shown in Fig. 2(a). It has the same Cartesian coordinates as these shown in Fig. 1(a). We assume that the silica probe has a uniform diameter of 500 nm in a 2-μm length, the photoresist coated on the silicon substrate has a thickness of 100 nm, and the probe contacts with the photoresist surface at a angle of 5°. The refractive index of air is assumed to be 1.0, and the refractive indices of silica, silicon, and photoresist are 1.47, 4.76, and 1.69 at 442 nm, respectively. Figures 2(b)–(d) show three calculated components of Poynting vector in the middle plane of the photoresist layer. The three components are alone X, Y, Z axis respectively and are normalized by the light source. As we can see, almost all of the energy is within the width of 1 μm, so the submicron line is easily exposed by this highly confined energy.

The direct writing samples using the submicron-diameter fiber are characterized by scanning electron microscopy (SEM) and atom force microscopy (AFM). Figure 3(a) shows SEM image of lines written by the submicron-diameter fiber probe shown in Fig. 1(b). The writing parameters of all lines are the same: writing speed of 16 μm/s and probe output power of 40 nW. The width of a single line is 510 nm, as shown in the inset of Fig. 3(a). Figure 3(b) shows the cross section profile of the lines measured by AFM. The depth of the line marked by the triangle is 117 nm. It is obvious that the whole depth of the photoresist layer is exposed.

Figure 4(a) is the SEM image of lines written by the same probe as Fig. 3 at different speeds. The output power of probe (50 nW) is fixed. The writing speeds of the lines from left to right are 20, 12, 12, and 9 μm/s, respectively, and the widths of corresponding lines are 380, 680, 680, and 850 nm, respectively. The faster writing speed provides the lower exposure dose, so that the two sides of the light fields with lower power (Fig. 2) cannot expose the photoresist. Therefore, the faster writing speed results in the thinner line. The thinnest line is 380 nm in width, which is smaller than the exposure wavelength of 442 nm. Moreover, the two middle lines demonstrate that the same writing speeds can keep the widths of different lines stable. Figure 4(b) shows the cross section profile of these lines measured by AFM. The depth of the line marked by the triangle is 116 nm.

Although the exposure dose can change the line width, the minimum width is limited by the output pattern of

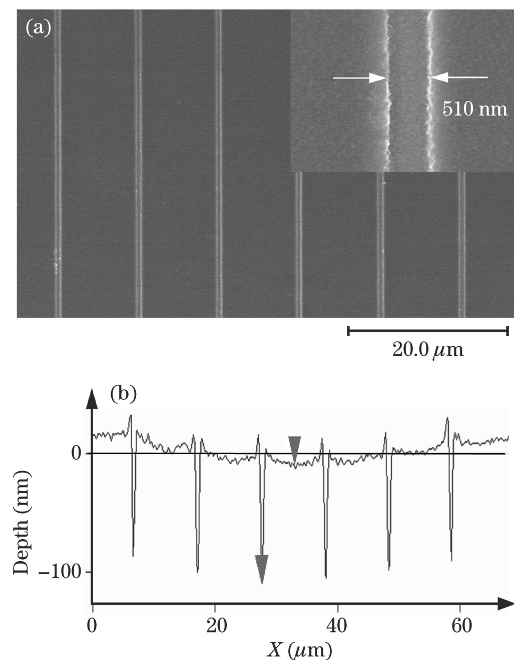

Fig. 3. (a) SEM image of the lines written by submicron-diameter fiber with 16-μm/s writing speed and 40-nW probe output power; (b) cross section profile of these lines measured by AFM.

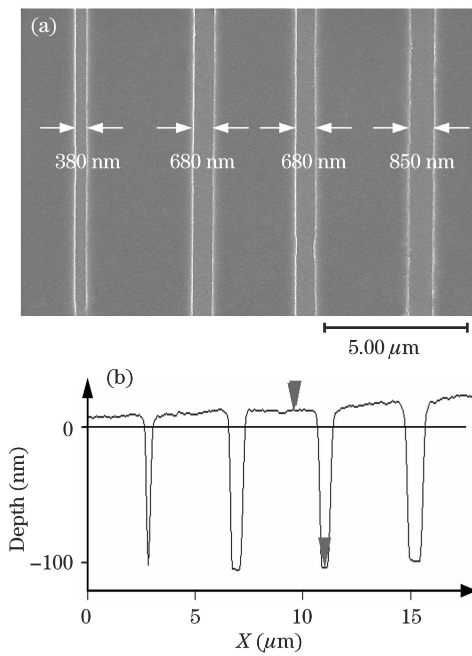

Fig. 4. (a) SEM image of the lines written by submicron-diameter fiber at different speeds. The writing speeds of these lines from left to right are 20, 12, 12, and 9 μm/s, respectively. Probe output power is 50 nW; (b) cross section profile of these lines measured by AFM.

submicron-diameter fiber. Wang *et al.* has numerically calculated the output patterns of micro- and nano-fibers using a FDTD method[17]. The results show that the beam width of near-field output can be tuned by the ratio of fiber diameter and light wavelength, and there is a certain value of the ratio with which the submicron-fiber emits light with the lowest divergence in the near field[17]. Therefore, if submicron-diameter fiber probe is optimized, the lines written by this method will be thinner.

In addition, by altering the writing direction of lines, complex submicron patterns can be fabricated. It needs a rotation stage fixed on the translation stage, and the probe tip must be aligned with the rotation axis to avoid the lines' deviation caused by rotation. The probe tip can coincide with the center of rotation stage under the monitoring of two orthogonal microscope cameras. When the substrate is rotated, the lines with different directions can be written.

In conclusion, a direct writing technique using submicron-diameter fibers has been presented. Using this technique, the submicron lines with different widths can be obtained. Its resolution can be smaller than the exposure wavelength. Besides high resolution, simple, and efficient process makes it promising for the future applications. By altering the writing direction of lines, complex submicron patterns can be fabricated.

This work was supported by the National Natural Science Foundation of China under Grant Nos. 60778030 and 60678037.

References

1. L. Zhang, C. Li, W. Liu, L. Zhou, G. Wu, and D. Wang, Acta Opt. Sin. (in Chinese) **26,** 1048 (2006).
2. H. Yang, M. Zhou, J. Dai, J. Di, and E. Zhao, Chin. Opt. Lett. **6,** 864 (2008).
3. S. A. Slattery, D. N. Nikogosyan, and G. Brambilla, J. Opt. Soc. Am. B **22,** 354 (2005).
4. H. C. Tapalian, J. Langseth, Y. Chen, J. W. Anderegg, and J. Shinar, Appl. Phys. Lett. **93,** 243304 (2008).
5. Y. Wu, C. Wang, W. Jia, X. Ni, M. Hu, and L. Chai, Chin. Opt. Lett. **6,** 51 (2008).
6. Z. Jin, J. Tan, S. Zhang, and L. Wang, Acta Opt. Sin. (in Chinese) **28,** 1730 (2008).
7. Y. Li, D. Chen, J. Zhu, C. Yang, and Y. Kanamori, Acta Opt. Sin. (in Chinese) **22,** 1008 (2002).
8. L. Tong, R. R. Gattass, J. B. Ashcom, S. He, J. Lou, M. Shen, I. Maxwell, and E. Mazur, Nature **426,** 816 (2003).
9. L. Tong, J. Lou, and E. Mazur, Opt. Express **12,** 1025 (2004).
10. M. Wu, W. Huang, and L. Wang, Chin. Opt. Lett. **6,** 732 (2008).
11. W. Liang, Y. Huang, Y. Xu, R. K. Lee, and A. Yariv, Appl. Phys. Lett. **86,** 151122 (2005).
12. Y. Li and L. Tong, Opt. Lett. **33,** 303 (2008).
13. X. Jiang, Y. Chen, G. Vienne, and L. Tong, Opt. Lett. **32,** 1710 (2007).
14. M. Sumetsky, Y. Dulashko, J. M. Fini, and A. Hale, Appl. Phys. Lett. **86,** 161108 (2005).
15. X. Jiang, Q. Yang, G. Vienne, Y. Li, L. Tong, J. Zhang, and L. Hu, Appl. Phys. Lett. **89,** 143513 (2006).
16. I. I. Smolyaninov, D. L. Mazzoni, and C. C. Davis, Appl. Phys. Lett. **67,** 3859 (1995).
17. S.-S. Wang, J. Fu, M. Qiu, K.-J. Huang, Z. Ma, and L.-M. Tong, Opt. Express **16,** 8887 (2008).